GSK3 and Polo-like kinase regulate ADAM13 function during cranial neural crest cell migration

Genevieve Abbruzzese*, Hélène Cousin*, Ana Maria Salicioni, and Dominique Alfandari
Department of Veterinary and Animal Sciences, University of Massachusetts, Amherst, MA 01003

ABSTRACT **ADAMs are cell surface metalloproteases that control multiple biological processes by cleaving signaling and adhesion molecules. ADAM13 controls cranial neural crest (CNC) cell migration both by cleaving cadherin-11 to release a promigratory extracellular fragment and by controlling expression of multiple genes via its cytoplasmic domain. The latter activity is regulated by γ-secretase cleavage and the translocation of the cytoplasmic domain into the nucleus. One of the genes regulated by ADAM13, the protease calpain8, is essential for CNC migration. Although the nuclear function of ADAM13 is evolutionarily conserved, it is unclear whether the transcriptional regulation is also performed by other ADAMs and how this process may be regulated. We show that ADAM13 function to promote CNC migration is regulated by two phosphorylation events involving GSK3 and Polo-like kinase (Plk). We further show that inhibition of either kinase blocks CNC migration and that the respective phosphomimetic forms of ADAM13 can rescue these inhibitions. However, these phosphorylations are not required for ADAM13 proteolysis of its substrates, γ-secretase cleavage, or nuclear translocation of its cytoplasmic domain. Of significance, migration of the CNC can be restored in the absence of Plk phosphorylation by expression of calpain-8a, pointing to impaired nuclear activity of ADAM13.**

Monitoring Editor
Marianne Bronner
California Institute of Technology

Received: May 12, 2014
Revised: Sep 25, 2014
Accepted: Sep 26, 2014

INTRODUCTION

Proteases of the family "a disintegrin and metalloprotease" (ADAM) are transmembrane proteases that play crucial roles during development and disease progression. They are the major protease family involved in the shedding of membrane-bound proteins (cleavage within the extracellular domain) and thus provide a means for rapidly modifying the level and function of proteins on the cell surface. Their shedding activity is central to the regulation of cell–cell and cell–substratum adhesion, as well as critical signaling pathways such as Notch, epidermal growth factor (EGF), Eph/ephrin, and Wnt. This can control various cell processes, such as fate determination, growth, survival, and migration (Alfandari *et al.*, 2009).

We previously showed that in *Xenopus laevis*, the meltrin ADAMs 9, 13, and 19 all play important and partially overlapping roles in the cranial neural crest (CNC; McCusker *et al.*, 2009; Neuner *et al.*, 2009; Cousin *et al.*, 2011, 2012). The CNC is a group of stem cells that undergoes extensive migration in the embryo and gives rise to the various craniofacial structures of all gnathostomes, including bones, cartilage, and cranial ganglia (Santagati and Rijli, 2003). We showed that ADAM13 plays a dual role in CNC migration. On the cell surface, ADAM9 and ADAM13 are both capable of cleaving the cell adhesion molecule cadherin-11 to release its adhesive extracellular domain to stimulate migration (McCusker *et al.*, 2009). Intracellularly, the ADAM13 cytoplasmic domain possesses a surprising ability to control gene expression when it is cleaved from the membrane-bound protease by γ-secretase and shuttled to the nucleus. The cytoplasmic domains of ADAM13 and 19 can both activate the expression of the cytoplasmic protease calpain8-a, and this is required for CNC migration (Cousin *et al.*, 2011). Nuclear translocation is also seen for the cytosolic tail of human ADAM10 and is believed to contribute to prostate cancer progression, suggesting that

This article was published online ahead of print in MBoC in Press (http://www.molbiolcell.org/cgi/doi/10.1091/mbc.E14-05-0970) on October 8, 2014.

*These authors contributed equally to this work

G.A., H.C., and D.A. designed the experiments and contributed to manuscript preparation. G.A. and H.C. performed the experiments. A.M.S. contributed to the GSK3 and Plk kinase assays.

Address correspondence to: Dominique Alfandari (alfandar@vasci.umass.edu).

Abbreviations used: ADAM, a disintegrin and metalloprotease; CNC, cranial neural crest; EGF, epidermal growth factor; GFP, green fluorescent protein; GSK-DN, GSK3-dominant negative; GSK3, glycogen synthase kinase 3; IP, immunoprecipitation; ISH, in situ hybridization; MBS, modified Barth's saline; MO, morpholino oligonucleotide; nCherry, nuclear Cherry; NI, noninjected; PKC, protein kinase C; Plk, Polo-like kinase; Plk-DN, Plk-dominant negative; RFP, red fluorescent protein.

an independent function for the ADAM cytoplasmic domain separate from the metalloprotease activity may be a conserved feature among ADAMs (Arima *et al.*, 2007; Tousseyn *et al.*, 2009). In addition to its role in regulating gene expression, the cytoplasmic domain of ADAM13 also regulates its own protein level (Alfandari *et al.*, 2001) and binds to the SH3-containing protein PACSIN2, which appears to negatively regulate ADAM13 activity in vivo (Cousin *et al.*, 2000).

Phosphorylation of the cytoplasmic domain has been implicated in regulating the function of several ADAMs, although these studies mainly focused on the mechanism of controlling the proteolytic activity. For example, the ADAM9 cytoplasmic domain can bind to and be phosphorylated by protein kinase C δ (PKCδ), and the activation of PKC by phorbol ester stimulates ADAM9 shedding of HB-EGF (Izumi *et al.*, 1998). In addition, in response to either PKC activation or growth factor stimulation, ADAM17 is phosphorylated by extracellular signal-regulated kinase (ERK), and this is required for efficient ectodomain shedding of the TrkA receptor tyrosine kinase by ADAM17 (Diaz-Rodriguez *et al.*, 2002; Soond *et al.*, 2005). It is not clear how these phosphorylation events regulate ADAM function and whether they serve to directly modify the enzymatic activity of the protease or mediate interactions with intracellular binding partners.

ADAM13 contains multiple predicted kinase target sites within the cytoplasmic domain, including Polo-like kinase (Plk) and glycogen synthase kinase 3 (GSK3). Plk is a well-conserved serine/threonine kinase family containing five members (Plk1–5) that has traditionally been studied for activities in cell cycle progression, such as promoting spindle assembly and centrosome maturation (Petronczki *et al.*, 2008; Stuhlmiller and Garcia-Castro, 2012). However, more recently, Plks have been noticed for nonproliferative functions, such as neuronal differentiation and synaptic homeostasis (de Carcer *et al.*, 2011), as well as cell migration and invasion of breast cancer cells (Rizki *et al.*, 2007). GSK3, which includes the α and β isoforms, is also a serine/threonine kinase with many cellular substrates and can affect diverse cell processes, such as apoptosis, cell cycle, cell polarity, and migration (Doble and Woodgett, 2003; Sun *et al.*, 2009). It participates in multiple signaling pathways, including canonical Wnt signaling, which is known to play a role in the specification of the CNC (Stuhlmiller and Garcia-Castro, 2012).

In this study, we identify novel roles for Plk and GSK3 in the CNC and show that decreasing the activity of either kinase inhibits cell migration in vivo. Our findings suggest that ADAM13 is an important substrate and is phosphorylated by GSK3 at two sites (serines 752 and 768) and by Plk at threonine 833. Kinase regulation at these residues is not required to induce ectodomain shedding by ADAM13 but does appear to be important for the nuclear function of ADAM13. In the absence of phosphorylation at the Plk site, CNC cell migration can be recovered by increasing the transcript levels of the critical target gene calpain8-a, indicating that phosphoregulation plays a significant role in the intracellular signaling activity of ADAM13.

RESULTS

ADAM13 phosphorylation sites are critical during CNC migration

To better understand how ADAM13 function is regulated, we identified several putative phosphorylation sites within the cytoplasmic domain using protein prediction software (ELM; Dinkel *et al.*, 2014). To ask whether phosphorylation at any of these sites is functionally important for ADAM13 activity during CNC migration, we replaced

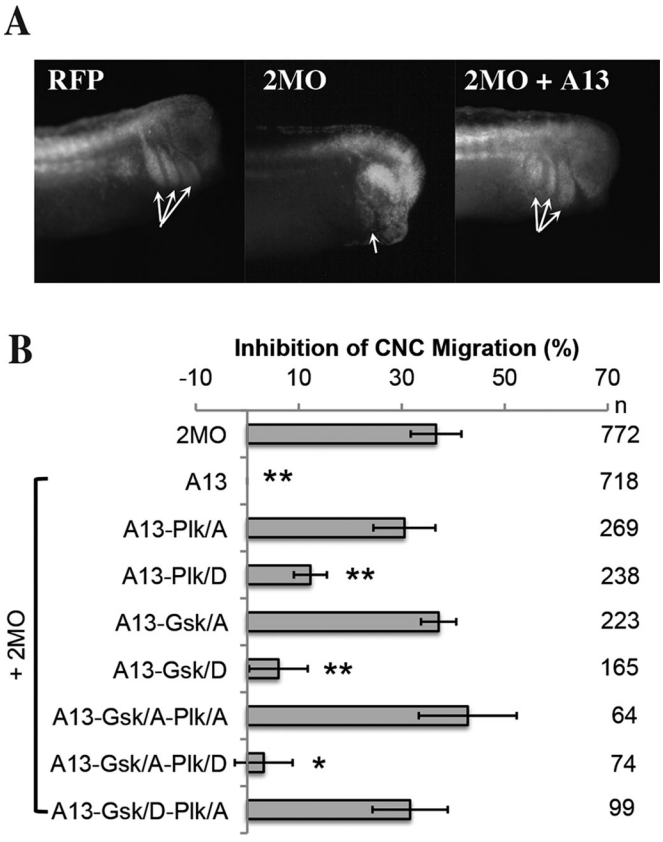

FIGURE 1: Phosphorylation sites are required for ADAM13 function during CNC migration. (A) Fluorescence images showing representative embryos for the injections of RFP alone, the knockdown with 2MO, or the rescue with wild-type ADAM13. Arrows indicate the position of the three migration segments (from left to right: hyoid, branchial, mandibular). (B) Histogram of targeted injection assays testing the ability of ADAM13 phosphomutants to rescue CNC migration in ADAM13/19-deficient embryos (2MO) from at least three independent experiments. Values are percentages of embryos with no CNC migration, normalized to 2MO + wild-type ADAM13. The error bars correspond to the SD. *n*, number of embryos scored for each case. Statistical significance of rescue: $*p < 0.05$, $**p < 0.01$.

the specific residues with either an alanine to prevent phosphorylation or a negatively charged aspartate to mimic constitutive phosphorylation. We chose targeted injection as the most direct technique to test the ability of these variants to replace the function of endogenous ADAM13 in the CNC (Figure 1A). In this technique, a single CNC precursor cell is injected with red fluorescent protein (RFP) as a lineage tracer to follow migration in vivo (McCusker *et al.*, 2009). In these experiments, percentage inhibition represents the percentage of embryos without CNC migration rather than a decrease in migration length, which can be subjective. Because cleavage patterns can vary in different batches of embryos, we used RFP alone in each experiment to determine the targeting efficiency and normalized the results. In each experiment, the ability of the mutant to rescue migration was compared with wild-type ADAM13. For this assay, we knocked down both ADAM13 and ADAM19 using morpholino oligonucleotides (MOs), since we have shown that the cytoplasmic domains of these ADAMs have overlapping functions and can regulate calpain8-a gene expression to stimulate migration (Cousin *et al.*, 2011). Our results show that replacing ADAM13 with nonphosphorylatable constructs for the GSK3 (A13-Gsk/A) or the

Plk sites (A13-Plk/A) did not rescue CNC migration in morphant embryos. Conversely, the phosphomimetic for either of these sites (A13-Gsk/D or A13-Plk/D, respectively) is able to significantly rescue migration (Figure 1B and Supplemental Figure S1). This suggests that phosphorylation at the GSK3 and Plk sites is essential for ADAM13 function in the CNC.

The binding of Plk to its substrate often requires that the substrate first be phosphorylated at the sequence Ser-(pSer/pThr)-(Pro/X). Once bound to its phospho-primed substrate, Plk will phosphorylate it at a different locus (Elia *et al.*, 2003). Of interest, ADAM13 contains three of these consensus motifs, two of which are also the putative GSK3 target sites. Therefore we generated complementary amino acid substitutions that would block phosphorylation at one site (GSK3 or Plk) while mimicking phosphorylation at the other to determine whether the GSK3 and Plk phosphorylation sites are functionally linked or independent. These data show that mimicking phosphorylation at the GSK3 sites is not sufficient to rescue ADAM13 function when the Plk phosphorylation site is blocked (A13-Gsk/D-Plk/A; Figure 1B). However, the phosphomimetic Plk site is capable of rescuing the nonphosphorylatable GSK3 sites (A13-Gsk/A-Plk/D).

To confirm the migration results, we also performed in situ hybridization (ISH) on embryos injected with the two morpholinos (MO13 and MO19 [2MO]) at the one-cell stage and further injected at the eight-cell stage with the various ADAM13 constructs. Embryos were sorted left and right before ISH using the fluorescent lineage tracer coinjected with the rescue mRNA. We used a combination of Sox10 and Twist probes to detect early- and late-migrating cells, respectively. To our surprise, most of the embryos showed a relatively normal positioning of CNC (Supplemental Figure S2). We then measured the length of CNC segments on both sides of each embryo and scored the number of embryos in which the length varied by >20% on the side injected with mRNA compared with the contralateral side with 2MO alone (Supplemental Figure S2; green, increase in segment length; red, decrease in segment length). The results obtained for A13-Plk/D (rescue), A13-Gsk/A (no rescue), and A13-Gsk/D (rescue) were all consistent with the targeted injection results, whereas the results using A13-Plk/A were not (equal number of rescue and worsening of the phenotype).

To understand why the ISH results did not show the obvious CNC positioning defect, we performed grafts with CNC lacking ADAM13 and 19 and expressing the A13-Plk/A mutant. As seen for the targeted injections, CNC migration was not observed in these grafts (Supplemental Figure S3A). We then fixed the embryos and performed ISH. The results show that even in these embryos in which the grafted CNC did not migrate, the overall ISH pattern was mostly normal (Supplemental Figure S3B). Collectively these results show that ISH is not always a reliable method to measure cell migration (see *Discussion*) and that, when possible, analysis of lineage tracer should be used.

We then tested, first, whether the two kinases were present in the CNC and, second, whether they could phosphorylate ADAM13. To answer the first question, we performed a Western blot on CNC dissected at stage 17 using antibodies specific to either kinase. Indeed, each antibody detected the predicted size band (Figure 2A), demonstrating that both GSK3 and Plk proteins are present in the CNC during migration. We then produced an antibody against a phosphorylated peptide corresponding to the Plk site in ADAM13. The antibody was affinity purified against the phosphorylated peptide and affinity depleted with the nonphosphorylated peptide. Human HEK293T cells were transfected with either the wild-type ADAM13 or the nonphosphorylatable mutant A13-Plk/A. We found that wild-type ADAM13 was clearly phosphorylated in these cells, whereas the mutant was not (Figure 2B). In addition, treatment of the cells with either a Plk inhibitor or a GSK3 inhibitor prevented this phosphorylation, showing that in HEK293T cells, endogenous Plk did phosphorylate ADAM13. This further suggests that in the absence of GSK3, Plk did not phosphorylate ADAM13. Of interest, in these cells, the main form of ADAM13 phosphorylated is shorter (~65 kDa) than the mature ADAM13 (M; 100 kDa), suggesting that this form may not contain the metalloprotease domain (form D). This shorter form of ADAM13 is also the one phosphorylated in vitro by purified

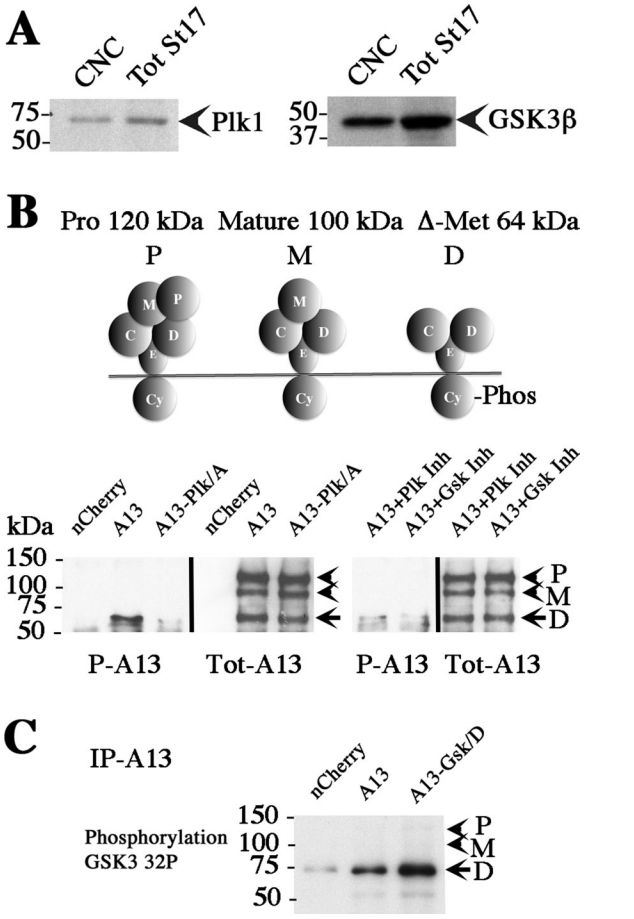

FIGURE 2: GSK3 and Plk can phosphorylate ADAM13. (A) Western blots for Plk1 (68 kDa) and GSK3β (47 kDa) on protein extract from 27 dissected CNC (CNC) or one total embryo equivalent at the same stage as dissection (Tot St17). (B) Western blot showing phosphorylation of ADAM13. The main forms of ADAM13 protein are represented at the top. The pro form (P) contains the prodomain and is inactive, the mature form (M) is proteolytically active, and cleavage of the metalloprotease domain results in a shorter form (D) that appears to be the principal phosphorylated form of ADAM13. Nuclear Cherry (nCherry, negative control), ADAM13 (A13), or the nonphosphorylatable mutant (A13-Plk/A) was expressed in HEK293T cells. Cells expressing ADAM13 were treated overnight with dimethyl sulfoxide (DMSO), Plk inhibitor (Plk Inh), or GSK3 inhibitor (Gsk Inh). All of the samples were first immunoprecipitated with a monoclonal antibody to ADAM13 (mAb 4A7), followed by Western blot using the phospho-ADAM13 antibody to the Plk phosphorylation site (P-A13) or the rabbit polyclonal to the ADAM13 cytoplasmic domain 15F for the total ADAM13 protein (Tot). (C) Autoradiograph of immunoprecipitated ADAM13 produced in HEK293T cells phosphorylated by purified active GSK3.

GSK3 (Figure 2C). Phosphorylation was increased in the ADAM13 mutant A13-Gsk/D, suggesting that the third GSK3 phosphorylation site (885T) of ADAM13 can also be phosphorylated in vitro.

GSK3 and Plk activity are required for ADAM13 function in CNC migration

Our mutation analysis suggests that GSK3 and Polo kinases should be required for CNC migration at least to phosphorylate ADAM13. Because these kinases are critical in multiple biological processes, we next tested whether lowering their activity in the CNC would cause a defect in migration without other major developmental defects. In particular, GSK3 was shown to phosphorylate the transcription factor Twist to modify its activity (Lander *et al.*, 2013). A nonphosphorylatable form of Twist did not bind to and inhibit Slug/Snail2, suggesting that phosphorylation by GSK3 is critical for normal Twist function during CNC development. To lower each kinase activity, we used previously characterized dominant-negative constructs and tested their ability to interfere with CNC migration without inhibiting CNC induction when injected at relatively low doses. Our results show that 300 pg of the GSK3 dominant negative (GSK3-DN; Dominguez *et al.*, 1995) injected at the eight-cell stage in a CNC precursor perturbed CNC migration in 30% of the injected embryos, whereas it did not perturb the expression of Slug in premigratory CNC (Figure 3). We also performed grafts on embryos injected with the dominant-negative GSK3 that confirmed that migration was inhibited in these embryos (Supplemental Movie S1). We then coinjected either wild-type or the phosphomimetic forms of ADAM13 together with the GSK3-DN to test their ability to rescue migration. We found that expressing both ADAM13-Gsk/D and -Plk/D, but not the wild-type ADAM13, could rescue the loss of migration caused by GSK3-DN (Figure 3, B and C). This confirms that one of the key substrates of GSK3 during CNC migration is ADAM13 and that phosphorylations at the GSK3 and Plk sites are required for proper ADAM13 function in vivo.

We next tested the requirement of Plk in CNC induction and migration using low doses of a dominant-negative construct, Plk-DN (Descombes and Nigg, 1998). Decreasing Plk activity by injecting 80 pg of Plk-DN mRNA at the eight-cell stage led to 52% inhibition of CNC cell migration (Figure 4A and Supplemental Movie S2). We then asked whether this migration defect could be rescued by coexpressing the ADAM13 phosphomimetic variants. In contrast to GSK3-DN, which was rescued by both phosphomimetics (Figure 3B), only the Plk-mimetic, A13-Plk/D, could restore migration of the CNC when Plk activity was reduced (Figure 4A). This is consistent with a model of successive phosphorylation of ADAM13 cytoplasmic domain by which Plk functions downstream of GSK3. To confirm the effect of Plk-DN on migration, we also performed in situ hybridization to detect the CNC markers Twist and Sox10 and observed similar results to those obtained by fluorescence in the targeted injection assays. We found that whereas CNC induction appeared unaffected by Plk-DN, there was a defect in migration caused by decreasing Plk activity, and this could be rescued by coexpressing ADAM13-Plk/D (Figure 4, B and C). Taken together, these results suggest that during CNC migration, ADAM13 is regulated by Plk and GSK3 phosphorylation and that the Plk phosphorylation is absolutely required, whereas GSK3 phosphorylation can be omitted if the Plk site is phosphorylated.

ADAM13 protease activity is not regulated by GSK3 or Plk phosphorylation

To determine the effect of GSK3 and Plk phosphorylations on ADAM13 proteolytic activity, we tested the ability of the nonphosphorylatable mutants to cleave substrates both in vitro and in vivo. When cotransfected with the protocadherin PAPC in Cos-7 cells, both nonphosphorylatable ADAM13 variants Plk/A and Gsk/A are able to shed the extracellular domain of PAPC from the cell surface as efficiently as wild-type ADAM13, whereas the protease active-site mutant ADAM13-E/A cannot (Cousin *et al.*, 2011; Figure 5A). Similarly, the phosphodeficient variants are also able to undergo

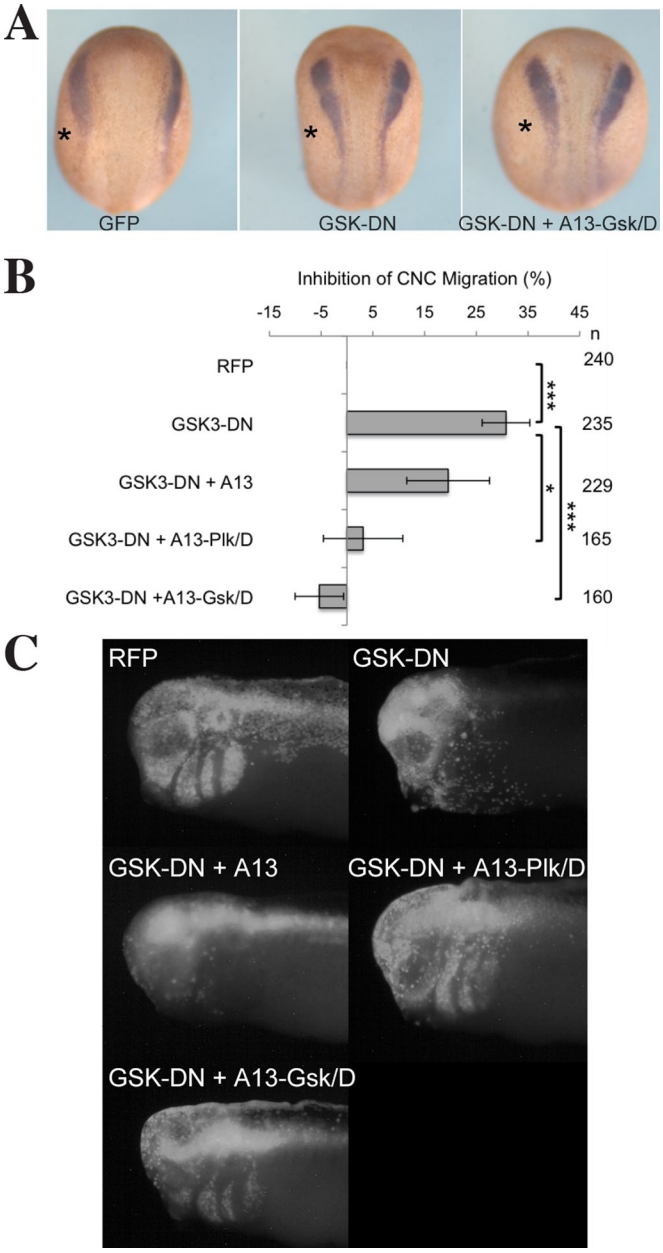

FIGURE 3: GSK3 activity is critical for ADAM13 in CNC cell migration. (A) In situ hybridization using a probe to detect the CNC marker slug in neurula-stage embryos (st. 14), showing that induction is not affected by GSK3-DN. Injected sides of each embryo are on the left (asterisk). (B) Histogram representing the percentage of embryos with no CNC migration in a targeted injection assay from at least five independent experiments. Values are normalized to injection of RFP alone. Error bars are SD. *n*, number of embryos scored. *$p < 0.01$, ***$p < 0.001$. (C) Fluorescence images showing typical result for each case in the targeted injection assay in B. A defect in migration is scored by the absence of RFP-labeled cells within the migration pathway.

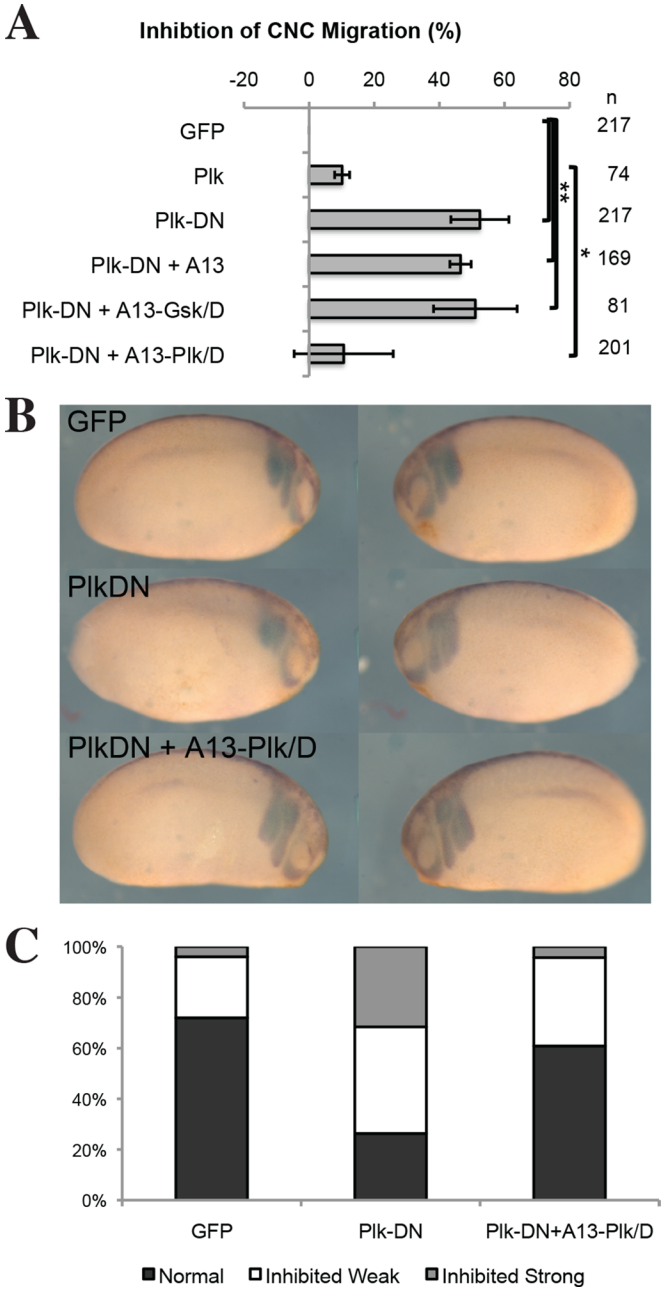

FIGURE 4: ADAM13 requires Plk activity in the CNC. (A) Histogram showing the percentage of embryos with inhibited CNC migration in a targeted injection assay. Values are normalized to injection of GFP alone and are from at least three independent experiments. Error bars are SD. *n*, number of embryos scored. $*p < 0.05$, $**p < 0.01$. (B) In situ hybridization detecting both of the CNC markers Sox10 and Twist in early tailbud embryos (st. 21), showing that migration, but not induction, is decreased by Plk-DN. Injected side of each embryo is on the left. (C) Analysis of CNC migration from the in situ hybridizations in B, showing the percentage of embryos for each case with severe, weak, or no defect in CNC migration on the injected side compared with the noninjected side of each embryo.

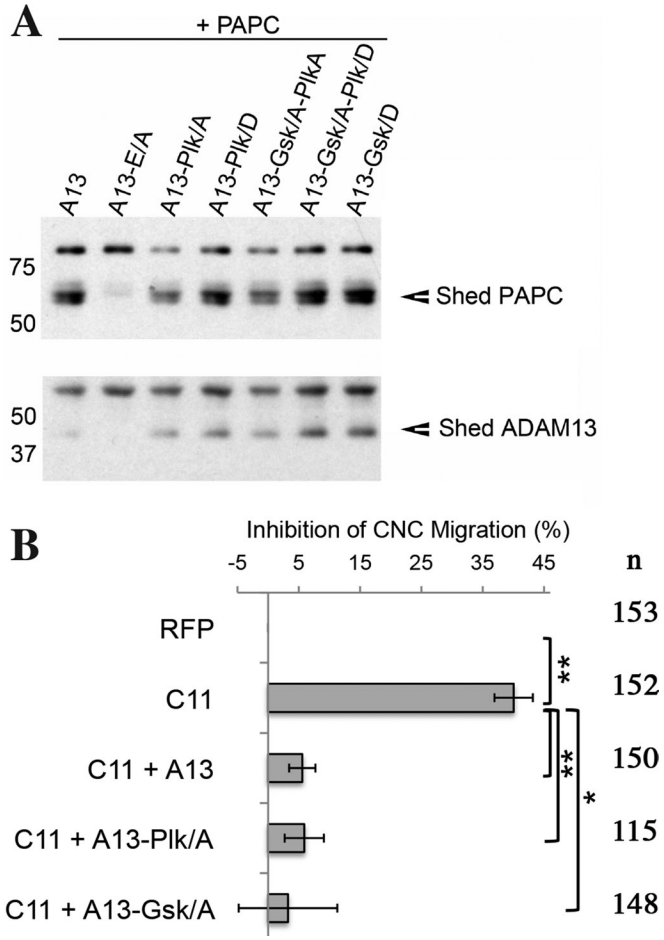

FIGURE 5: Phosphorylation of ADAM13 does not affect its proteolytic activity. (A) Western blot from Cos-7 cells transfected with the protocadherin PAPC and various ADAM13 constructs. The glycoproteins purified from the conditioned media were probed with an antibody to the extracellular domain of PAPC or with 7C9, a monoclonal antibody to the cysteine-rich domain of ADAM13. E/A is a catalytically inactive variant of ADAM13. (B) The histogram represents the percentage of embryos displaying no migration from targeted injection of cadherin-11 mRNA alone or together with the ADAM13 variants. Values are normalized to RFP alone. Error bars are SD. *n*, number of embryos scored from at least three independent experiments. $*p < 0.05$, $**p < 0.01$.

autoproteolysis to shed their own ectodomain into the medium (Gaultier *et al.*, 2002; Figure 5A). In addition, coexpressing Plk-DN or GSK3-DN does not prevent wild-type ADAM13 from shedding PAPC (unpublished data).

To examine ADAM13 protease activity in vivo, we used the targeted injection assay to overexpress the phosphodeficient variants along with the cell adhesion molecule cadherin-11 in the CNC. Overexpression of cadherin-11 prevents CNC migration, and this can be rescued by coexpression of either ADAM13 or the extracellular fragment of cadherin-11 (McCusker *et al.*, 2009). Accordingly, whereas cadherin-11 blocked migration in 40% of embryos, both the A13-Plk/A and -Gsk/A variants could rescue migration as efficiently as wild-type ADAM13 (Figure 5B). The results from these in vitro and in vivo assays indicate that phosphorylation of ADAM13 by GSK3 and Plk is not essential for the proteolytic cleavage of at least two of its identified substrates, PAPC and cadherin-11.

Plk controls the nuclear function of ADAM13

The cleaved cytoplasmic domain of ADAM13 (C13) must translocate to the nucleus and increase calpain8-a (Capn8) expression to promote CNC migration (Cousin *et al.*, 2011). Therefore we investigated whether phosphorylation by Plk is necessary to stimulate the cleavage of C13 from the membrane-bound protease, its

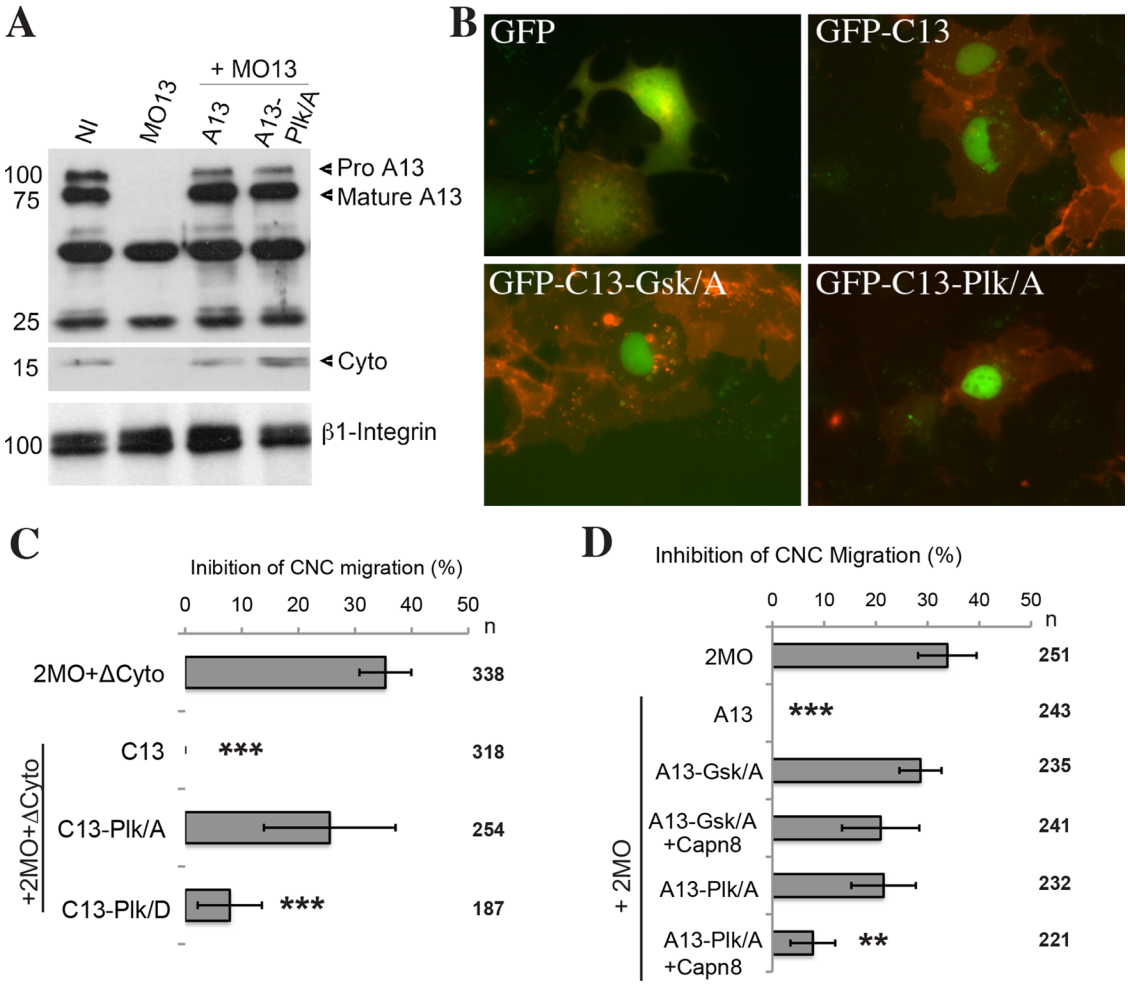

FIGURE 6: ADAM13-dependent regulation of calpain8 expression depends on ADAM13 phosphorylation. (A) ADAM13 was immunoprecipitated (IP) from 20 embryos using a goat polyclonal antibody g821. Noninjected embryos (NI) at stage 18 (neurula) are compared with sibling embryos injected with MO13 or MO13 plus MO-resistant mRNA encoding ADAM13-Plk/A or wild type. ADAM13 protein was detected by Western blot using 6615F. The polyvinylidene fluoride membrane was cut below 25 kDa and the two halves probed separately. The cleaved cytoplasmic domain (Cyto) is observed at 17 kDa for both wild-type and Plk/A ADAM13. Samples of the input for the IP were analyzed by Western blot with the 8C8 antibody for β1 integrin as a loading control. (B) Fluorescence images showing the localization of GFP-fusion proteins (green) expressed in Cos-7 cells along with membrane-bound mCherry (red). GFP is observed uniformly throughout the cytoplasm and nucleus, whereas GFP-C13 and the phosphodeficient mutants all accumulate strongly in the nucleus. (C, D) Analyses of targeted injection assays displaying the loss of CNC migration as a percentage of embryos. (C) MO13 + MO19 (2MO) was coinjected with mRNA encoding ADAM13 lacking its cytoplasmic domain (ΔCyto) plus either GFP-C13 wild type or phosphomutants. Values are normalized to the rescue with GFP-C13 wild type, and Student's *t* tests were performed to compare values to 2MO + ΔCyto. (D) 2MO was injected with ADAM13-Plk/A or ADAM13-Gsk/A mRNA alone or together with Capn8 mRNA. Inhibitions are normalized to RFP, and Student's *t* tests were performed against 2MO. Error bars are SD from four or more independent experiments. *n*, number of embryos scored. $^{**}p < 0.01$, $^{***}p < 0.005$.

nuclear translocation, or its activity in gene regulation. We first showed that the cytoplasmic domain of ADAM13-Plk/A is cleaved in embryos, indicating that intramembrane processing by γ-secretase is not dependent on phosphorylation by Plk (Figure 6A). We then generated the alanine substitutions at the GSK3 and Plk sites in a construct containing C13 fused to green fluorescent protein (GFP-C13) to observe their subcellular localization. When transfected into Cos-7 cells, we found that, similar to wild-type GFP-C13, both variants containing the nonphosphorylatable alanine substitutions, GFP-C13-Plk/A and GFP-C13-Gsk/A, accumulate in the nucleus (Figure 6B). Thus the requirements for nuclear translocation of C13 do not rely on phosphorylation at the GSK3 or Plk sites.

To test whether these cytoplasmic domain phosphomutants are functional in the CNC, we performed a targeted injection assay to replace endogenous ADAM13 with a version of ADAM13 missing its cytoplasmic domain (ADAM13-Δcyto) complemented with the different GFP-C13 variants. Similar to the behavior of full-length ADAM13, we found that only C13-Plk/D could rescue CNC migration as well as wild type, with no significant rescue when phosphorylation was abolished (C13-Plk/A). This confirms that Plk phosphorylation is needed for the function of C13, independent of its extracellular functions such as proteolytic activity.

Finally, we asked whether the role of Plk phosphorylation is to regulate the transcriptional activity of C13. We showed that in

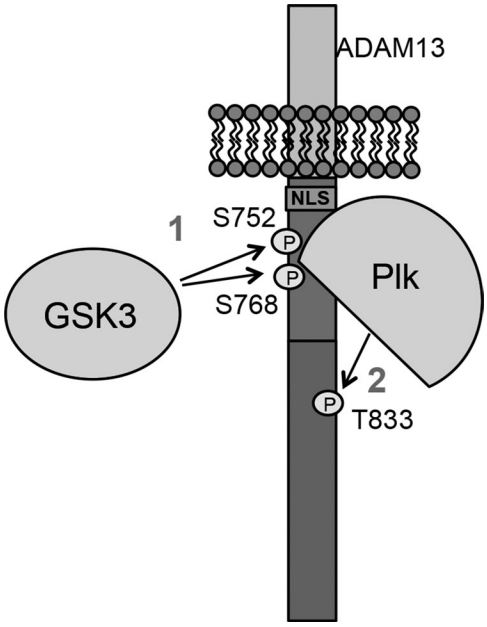

FIGURE 7: Successive phosphorylation of ADAM13. Proposed model depicting successive phosphorylation of ADAM13 by which GSK3 primes ADAM13 at two sites (S752 and S768; step 1) for subsequent phosphorylation at a second site on ADAM13 (T833; step 2). NLS, nuclear localization signal.

embryos lacking ADAM13 cytoplasmic domain, restoring the levels of Capn8 expression is sufficient to rescue CNC migration (Cousin *et al.*, 2011). This rescue is only possible if ADAM13 metalloprotease activity is also present. Therefore we tested whether expressing Capn8 mRNA could rescue the loss of migration in embryos expressing nonphosphorylatable ADAM13 with the two morpholinos against ADAM13 and 19 at the eight-cell stage. Capn8 expression was unable to rescue CNC migration when coexpressed with A13-Gsk/A. However, we observed partial but significant recovery when Capn8 was coexpressed with the A13-Plk/A mutant, which is consistent with the level of recovery obtained when coexpressed with ADAM13-Δcyto (Figure 6, C and D; Cousin *et al.*, 2011). These results suggest that phosphorylation of ADAM13 by Plk is important for its ability to regulate Capn8 transcript levels.

DISCUSSION

ADAM13 plays a central role in regulating cranial neural crest cell migration and induction in amphibian embryos (Alfandari *et al.*, 2001; Wei *et al.*, 2010; Cousin *et al.*, 2011, 2012). The cytoplasmic domain is critical, as it controls both the level of ADAM13 protein present in the CNC and the transcriptional activity in these cells (Cousin *et al.*, 2000; Cousin *et al.*, 2011). Here we show that one of these controls is mediated by a phosphorylation cascade involving GSK3 and Polo-like kinase. We further demonstrate that these phosphorylations, although essential for CNC migration, are not critical for ADAM13 cleavage of its extracellular substrates but are essential for the nuclear function of ADAM13. Our results suggest a model in which ADAM13 is successively phosphorylated in vivo, first by GSK3 to phosphoprime for Plk, and second by Plk at the critical residue T833 (Figure 7).

Phosphorylation of ADAM13 does not regulate proteolytic activity

ADAM phosphorylation has been shown to regulate either proteolytic activity or subcellular localization (Izumi *et al.*, 1998; Diaz-Rodriguez *et al.*, 2002; Soond *et al.*, 2005). Recently ADAM17 phosphorylation by Polo-like kinase 2 was shown to regulate the shedding of its substrate in mammalian cells (Schwarz *et al.*, 2014). In contrast, we show that ADAM13 proteolytic activity is not affected by its phosphorylation (Figure 5). Of importance, the level of protein expressed is not reduced in the nonphosphorylatable mutant, and the maturation and subcellular localization is indistinguishable from the wild-type protein (Figure 6, A and B).

To confirm that ADAM13 metalloprotease activity was unchanged in vivo, we tested the ability of nonphosphorylatable ADAM13 to rescue migration of CNC overexpressing cadherin-11 (Figure 5B). We and others have shown that increased cadherin-11 expression inhibits CNC migration (Borchers *et al.*, 2001; McCusker *et al.*, 2009) and that a corresponding increase of ADAM13 rescues migration by cleaving the excess cadherin-11. Here we show that the phosphodeficient ADAM13 can rescue cadherin-11 with the same efficiency as wild-type ADAM13 (Figure 5B). Finally, coexpression of the nonphosphorylatable cytoplasmic domain as a GFP fusion together with the extracellular and transmembrane domains of ADAM13 (with intact proteolytic activity) does not rescue CNC migration, whereas the wild-type cytoplasmic domain does (Figure 6C). This, together with the observation that the phosphorylated form does not appear to contain the metalloprotease domain (Figure 2B), confirms that these phosphorylations have no direct effect on the overall ADAM13 metalloprotease function and suggests that they are strictly involved with the nuclear function of the cytoplasmic domain of ADAM13 (Cousin *et al.*, 2011).

Phosphorylation of ADAM13 regulates its nuclear function

We previously identified a second and critical function for ADAM13 cytoplasmic domain. This function requires a sequence of events including the cleavage of the domain by γ-secretase and its translocation to the nucleus, where it regulates the expression of ~2000 genes (Cousin *et al.*, 2011). Among those targets, calpain-8a, a calcium-activated cytoplasmic protease, was shown to play an essential role in the migration process and to be able to compensate for the loss of the ADAM13 cytoplasmic domain (Cousin *et al.*, 2011). We show here that increasing the levels of calpain-8a expression can rescue migration of CNC expressing ADAM13-Plk/A, the mutant for the Plk phosphorylation site. The level of rescue was comparable to what was previously observed with a mutant of ADAM13 lacking the entire cytoplasmic domain (Cousin *et al.*, 2011). This suggests that the phosphorylation of ADAM13 by Plk is required to achieve the proper level of calpain-8a expression. On the other hand, calpain-8a expression had no effect by itself or when coinjected with the mutant for the GSK3 sites (Figure 6D; Cousin *et al.*, 2011). This suggests that Gsk3 phosphorylation of ADAM13 is important not only to create Plk-binding sites, but also for events downstream or parallel to calpain-8a transcription.

Calpain-8a is a cysteine protease, whose activity is tightly regulated by its level of RNA and subcellular localization and the concentration of calcium (Zanardelli *et al.*, 2013). Of interest, phosphorylation of ADAM13 by Plk is predicted to create a binding site for Forkhead association domain (FHA). Proteins that encode these domains, which were first identified in Forkhead transcription factors, have a wide range of activities, including gene regulation and DNA repair (Durocher *et al.*, 2000; Hammet *et al.*, 2003). For example, FoxK2, a transcription factor that is expressed in the *Xenopus* CNC

cells, contains one FHA domain (Pohl and Knochel, 2004). The analysis of the putative promoter region of calpain-8a in *Xenopus laevis* and *Xenopus tropicalis* revealed several conserved sites for FoxK2 within 1000 base pairs of the transcription start. It will be of interest to test whether ADAM13 binds to FoxK2 in vivo and whether this interaction modulates gene expression and controls CNC migration. Using mass spectrometry analysis, we identified several proteins that bind to the cytoplasmic domain of ADAM13 and the phosphomimetic A13-Plk/D but not to A13-Plk/A. Among these are proteins involved in cytoskeletal dynamics, DNA repair, and protein deacetylation. Additional work is required to sort out the relative contribution of these proteins in regard to ADAM13 nonproteolytic functions.

Another possibility is that calpain-8a is not localized or activated properly in the CNC expressing the nonphosphorylatable mutant. In that case, expression of more calpain-8a would compensate for a lower overall activity. For example, another member of the family, calpain-2, is required for proper convergent extension in the *Xenopus* gastrula and neurula (Zanardelli *et al.*, 2013). Its activity is tightly controlled by the noncanonical Wnt pathway. Wnt5a increases calpain-2 localization at the membrane, and this pathway is also known to regulate calcium concentration via PLC/IP3 activation. Both activities are regulated by Dishevelled, a protein that links the Frizzled receptor to the various cytoplasmic effectors. Multiple pieces of evidence suggest that ADAM13 is involved in the Wnt pathway and could therefore affect calpain-8a activity. First, in *X. tropicalis*, ADAM13 controls Wnt signaling by cleaving ephrinB1 and thus lowering the inhibition of the ephrin signaling on the Wnt pathway (Wei *et al.*, 2010). In *X. laevis*, ADAM13 binds and cleaves cadherin-11 and PAPC, which are also known to regulate the Wnt pathway (Jung *et al.*, 2011; Kietzmann *et al.*, 2012; Becker *et al.*, 2013; Koehler *et al.*, 2013). In addition, we found that ADAM13 directly interacts with multiple Frizzled receptors (G. Abbruzzese, A. Gorny, H. Cousin, I. Kleino, LT Kaufmann, H. Steinbeisser, and D. Alfandari, unpublished data). The consequences of these interactions with ADAM13 on Wnt signaling, as well as the contribution of the various phosphorylations, are not known, but it is possible that the noncanonical Wnt pathway, by regulating the local calcium concentration, may regulate calpain-8a activity during CNC migration.

ADAM knockdown does not overtly perturb CNC marker position by ISH

Our results show that whereas the knockdown of ADAM13 and 19 clearly affects CNC migration when tested by targeted injections or grafts (this study; McCusker *et al.*, 2009; Cousin *et al.*, 2011, 2012), the position of CNC detected by ISH in morphant embryos appears relatively unchanged (Supplemental Figure S2A). The central question is whether ADAM13 and 19 are essential for CNC migration, as suggested by grafts and targeted injections, or are dispensable, as suggested by ISH experiments. Related to this question is why ISH is not able to detect the changes produced by the lack of ADAM13 and 19 that are so obvious in grafts. We and others previously showed that cadherin-11 overexpression inhibits CNC migration, but that in this case, CNC markers are turned off in the nonmigrating cells (Borchers *et al.*, 2001; McCusker *et al.*, 2009). This is due at least in part to the excess cadherin-11 cytoplasmic domain sequestering β-catenin at the membrane and preventing its signaling activity, including its activation of Twist expression (Borchers *et al.*, 2001). We also showed that the knockdown of ADAM13 results in an increase in cadherin-11 due to a lack of proteolysis (McCusker *et al.*, 2009). This suggests that CNC lacking ADAM13 may also turn off the expression of markers. On close examination of grafts from embryos lacking ADAM13 and 19 treated by ISH, we found that the main population of grafted CNC that did not migrate was not obviously stained by the combination of Sox10 and Twist probes (Supplemental Figure S3; see also Supplemental Figure S4, yellow oval). In addition, we previously showed that ADAM13 and 19 activity was essential in the leading CNC but that morphant cells could follow wild-type cells in grafts (Cousin *et al.*, 2012). Similarly, in chickens, ADAM13 is expressed more abundantly in the leading cells than in the followers (McLennan *et al.*, 2012). Thus it is likely that some CNCs do not depend on ADAM13 and 19 for their migration, and these would be clearly detected by ISH markers. Combined with the fact that the nonmigrating CNCs are not detected, this can explain why the pattern of CNCs appears normal in morphant embryos. A schematic drawing of this hypothesis is presented in Supplemental Figure S4. In this figure, it is also possible to detect a small population of RFP-expressing cells that migrated from the graft despite the absence of ADAM13 and 19 and overlap with the positive ISH staining (white arrowheads). This is consistent with the hypothesis that some CNCs do not require ADAM13 and 19. It is important to keep in mind that ISH detects cells expressing a given marker at a specific time, which in some cases can be extrapolated to measure cell movement but is never a direct visualization of cell migration. Thus, by using multiple different techniques, such as graft and targeted injection, can clearly demonstrate the role of proteins that have a subtle function during cell migration, such as ADAM13.

GSK3 and Polo-like kinase regulate CNC migration

Our study also shows that GSK3 and Plk are critical for CNC migration. GSK3 is a well-known inhibitor of the canonical Wnt pathway, where it phosphorylates β-catenin to induce its degradation. Both canonical and noncanonical Wnt have been shown to play roles in CNC induction and migration. In particular, Wnt signaling is essential for the induction of CNC (Garcia-Castro *et al.*, 2002; Abu-Elmagd *et al.*, 2006), but evidence suggests that it needs to be turned off during migration. Activating the Wnt pathway by either stimulating with Wnt-1 or inhibiting GSK3 with LiCl blocks trunk neural crest cell migration (de Melker *et al.*, 2004), whereas genetic knockout of GSK3 in mice leads to cleft palate, a defect generally due to cranial neural crest cell migration defects (Liu *et al.*, 2007). In *Xenopus*, GSK3 phosphorylation of Twist modifies its activity, promotes its binding to Slug, and results in the inhibition of Slug (Lander *et al.*, 2013). Slug is one of the first transcription factors induced in the CNC and is progressively turned off during migration. GSK3 phosphorylation of Twist may help further inhibit the remaining Slug protein activity during migration. Our rescue using ADAM13 phosphomimetic mutant suggests that GSK3 activity could be involved in part to activate one or more ADAMs required for neural crest cell migration in other species. In the chicken embryo, ADAM10 and ADAM19 cleave cadherin-6b during the exit of the trunk neural crest cells from the neural tube (Schiffmacher *et al.*, 2014). Because both of these ADAMs have also been found to produce a cleaved cytoplasmic domain that can translocate in the nucleus, it is tempting to speculate that a similar regulation by phosphorylation could be important (Arima *et al.*, 2007; Tousseyn *et al.*, 2009; Cousin *et al.*, 2011).

Although Plk regulates multiple aspects of development through its control of cell cycle progression, there is no evidence of its role in controlling cell migration in a developmental context. On the other hand, Plk1 was previously shown to be important for the invasion of breast cancer cells through a laminin-rich extracellular matrix by phosphorylating the intermediate filament protein vimentin, which

in turn regulates the level of β1 integrin on the cell surface (Rizki *et al.*, 2007). Implication of Plk in cancer cell migration and invasion is growing and extending to multiple cancer types, but the mechanism of action is not well understood, and in many studies, the increase in the number of cells invading could be the result of increases in cell proliferation due to Plk overexpression. One interesting possibility is that at least part of Plk stimulation of cell migration is via the phosphorylation of an ADAM in a mechanism similar to what we observed for ADAM13.

MATERIALS AND METHODS

Morpholinos and DNA constructs

Morpholino antisense oligonucleotides (GeneTools, Philomath, OR) against ADAM13 and ADAM19 were described previously (McCusker *et al.*, 2009; Neuner *et al.*, 2009). All of the ADAM13 constructs used for the CNC migration assays contain seven silent mutations in the morpholino-binding region so that it is resistant to the MO13. Phosphorylation mutations were introduced by site-directed mutagenesis to replace the putative phosphorylated residue with alanine or aspartate. The predicted GSK3 sites are serines 752 and 768, and the predicted Plk site is threonine 833. Dominant-negative GSK3, containing the mutation K85R, has been characterized previously (Dominguez *et al.*, 1995) and was a generous gift from Isabel Dominguez (Boston University School of Medicine). The dominant-negative Plk construct (encoding the two Polo box domains of Plk1) was published previously (Ito *et al.*, 2008) and was a gift from Rafael Fissore (University of Massachusetts Amherst).

Antibodies

The following antibodies were used: g821, goat polyclonal antibody to the ADAM13 cytoplasmic domain (Cousin *et al.*, 2011); 6615F, rabbit polyclonal antibody to the ADAM13 cytoplasmic domain (Alfandari *et al.*, 1997); 4A7, mouse monoclonal to the ADAM13 cytoplasmic domain; 7C9, mouse monoclonal to the ADAM13 cysteine-rich domain (Gaultier *et al.*, 2002); PAPC, mouse monoclonal to the extracellular domain (Chen and Gumbiner, 2006), 8C8, monoclonal antibody to β1 integrin (Gawantka *et al.*, 1992); anti-Plk, mouse monoclonal to Plk1 (Invitrogen, Carlsbad, CA); and anti-GSK3, mouse monoclonal to GSK3 α/β (LifeSpan BioSciences, Seattle, WA). P-A13, the antibody to phosphorylated ADAM13 (833T, Plk site), was generated by immunizing two rabbits (ProSci, Poway, CA) with a phosphorylated peptide linked to KLH (EZBiolab, Carmel, CA). Phosphospecific antibodies were affinity purified on the phosphorylated peptide and immunodepleted using the non-phosphorylated peptide.

Injections

Capped mRNA were synthesized for all constructs except GSK3-DN using SP6 RNA polymerase on DNA linearized with *Not*I as described earlier (Cousin *et al.*, 2000). GSK3-DN was linearized with SacI and transcribed with T7 RNA polymerase. For the CNC targeted injection assays, embryos were injected at the eight-cell stage into either the left or right dorsal-animal blastomere (CNC precursor) with 200 pg of RFP or GFP mRNA as a lineage tracer. Morpholinos to ADAM13 and 19 (2MO, 1 ng each) were injected either alone or in combination with 80 pg of mRNA encoding wild-type ADAM13 or the various phosphomutants. 2MO plus ADAM13-Plk/A or A13-Gsk/A was rescued with 80 pg of calpain8-a mRNA. For the dominant negatives, 80 pg of Plk-DN mRNA was injected alone or together with 80 pg of ADAM13 mRNA, and 300 pg of GSK3-DN mRNA was injected alone or with 300 pg of ADAM13 mRNA. For the overexpression of cadherin-11, 300 pg of cadherin-11 and 300 pg of ADAM13 were used. Embryos were raised at 15°C until they reached tailbud stage (stages 24–27) and were scored for inhibition of CNC migration by the absence of RFP-positive cells within the migration pathways.

For in situ hybridizations, embryos were injected into one cell at the two-cell stage with 200 pg of GFP mRNA plus 300 pg of the mRNAs for Plk-DN, GSK3-DN, or ADAM13 variants. Embryos were sorted for RFP expression on the left or right side and fixed at neurula or early tailbud stage (14 or 21, respectively). Whole-mount in situ hybridizations were performed as described earlier (Harland, 1991). For ISH in Supplemental Figure S2, embryos were injected at the one-cell stage with MO13 and MO19 and then again at the eight-cell stage in one dorsal animal blastomere with RFP and the various ADAM13 constructs. Tailbud-stage embryos were sorted according to RFP expression in the left or right dorsal anterior tissue before ISH treatment. Quantification was performed by measuring the length of CNC segment on the injected side (rescue) and comparing it to the contralateral side. Embryos with a 20% increase or decrease in segment length were scored as rescued (green number) or worse (red number), respectively.

Grafts

Embryos were injected in one cell at the two-cell stage and raised at 14°C. Embryos were sorted for optimum lineage tracer expression (GFP or mRFP) at stage 15 (as soon as the anterior neural folds are visible and raised). The vitelline envelopes of selected embryos were removed, and embryos were placed in a dish of nontoxic modeling clay (Van Aken, Rancho Cucamonga, CA) containing 1× MBS (88.0 mM NaCl, 1.0 mM KCl, 2.4 mM $NaHCO_3$, 15.0 mM HEPES [pH 7.6], 0.3 mM $CaNO_3$-$4H_2O$, 0.41 mM $CaCl_2$-$6H_2O$, 0.82 mM $MgSO_4$) and 50 μg/ml gentamicin. Embryo-sized cavities were formed in the Plasticine using a Pasteur pipette whose tip had been melted into a glass ball. The embryos were placed in the cavities, oriented according to experimenter's grafting preference, and immobilized by pulling back some modeling clay around them. Once immobilized, the ectoderm covering the CNC was peeled off, the CNCs were cut out using an eyelash knife and hair loop, and grafted into host embryos whose CNCs were removed. Each CNC was grafted according to its proper anteroposterior and dorsoventral orientation. The grafted embryos were left to heal for 30 min in 1× MBS, with an embryo-sized coverslip pressed onto the dissected region of the embryo to maintain the ectoderm flush with the CNC and mesoderm. The embryos were then raised in a tissue culture dish coated with 1% agarose in 0.1× MBS and 50 μg/ml gentamicin at 14°C overnight.

Cell culture and transfection

293T cells were obtained from the American Type Culture Collection (ATCC, Manassas, VA) and transfected using X-tremeGENE HP according to manufacturer's instructions (Roche, Basel, Switzerland). For detection of phosphorylated ADAM13, cells expressing ADAM13 were treated overnight with 0.2% dimethyl sulfoxide, 0.1 μM Plk inhibitor GW843682X (Sigma-Aldrich, St. Louis, MO), or 1 μM GSK3 inhibitor AR-A014418 (Sigma-Aldrich). Cos-7 cells were obtained from ATCC and transfected using Fugene-6 (Roche) according to manufacturer's instruction. For PAPC and ADAM13 shedding assays, cells were incubated with medium containing 2% serum 24 h after transfection, and conditioned supernatants were collected at 48 h. The shed extracellular domains were purified using concanavalin-A–agarose (Vector Laboratories, Burlingame, CA) overnight, eluted in reducing Laemmli buffer, and blotted using the PAPC or 7C9 antibodies.

Immunoprecipitation and Western blots

Cells were extracted in RIPA buffer (Tris-buffered saline [TBS], 1% NP-40, 1% deoxycholate, 0.1% SDS) with protease phosphatase inhibitor cocktail (Pierce). Immunoprecipitation of ADAM13 was performed using a monoclonal antibody to the cytoplasmic domain (4A7), bound to protein G–agarose (Pierce Biotechnology, Rockford, IL), for 2 h at 20°C. Immunoprecipitates (IPs) were washed three times with extraction buffer before elution with Laemmli buffer. ADAM13 IPs were blotted using the phosphospecific antibody at 0.1 µg/ml overnight at 4°C. Unless otherwise noted, Western blots were performed on polyvinylidene fluoride membranes (Millipore, Billerica, MA) and blocked with 5% nonfat dry milk in TBS with 0.1% Tween-20. All antibody incubations and washes were also performed in TBS 0.1% Tween-20. Embryos for Western blots and immunoprecipitations were extracted in 1× MBS, 1% Triton X-100, 5 mM EDTA, and Halt Protease and Phosphatase inhibitor cocktail (ThermoScientific, Waltham, MA).

Kinase assays

For the in vitro phosphorylation, the 4A7 immunoprecipitates were washed in kinase buffer (25 mM 4-(2-hydroxyethyl)-1-piperazineethanesulfonic acid, pH 7.2, 10 mM $MgCl_2$, 10 mM $MnCl_2$, 1 mg/ml bovine serum albumin, 40 mM β-glycerophosphate, 5 mM *p*-nitrophenylphosphate, 10 µM aprotinin, and 10 µM leupeptin) and incubated with active GSK3 (SignalChem, Richmond, Canada) in the presence of ^{32}P-ATP as previously described (Li *et al.*, 2011).

Fluorescence microscopy

Cos-7 cells were transfected with the GFP-fusion proteins plus membrane-bound mCherry to visualize the cell boundaries and placed on fibronectin-coated (10 µg/ml) glass-bottom plates (MatTek, Ashland, MA). Photographs were taken using a Zeiss 200M inverted microscope equipped with an Apotome and a 63× oil immersion lens to obtain optical sections. For in vivo CNC migration assays, embryos were imaged using a Zeiss Stereo Lumar-V12 fluorescence microscope.

ACKNOWLEDGMENTS

We thank R. Fissore and I. Dominguez for helpful discussion and providing the Plk and GSK3 dominant-negative constructs. This work was supported by National Institutes of Health, U.S. Public Health Service, Grants F31-DE023275 to G.A. and RO1-DE016289 to D.A.

REFERENCES

Abu-Elmagd M, Garcia-Morales C, Wheeler GN (2006). Frizzled7 mediates canonical Wnt signaling in neural crest induction. Dev Biol 298, 285–298.

Alfandari D, Cousin H, Gaultier A, Smith K, White JM, Darribere T, DeSimone DW (2001). Xenopus ADAM 13 is a metalloprotease required for cranial neural crest-cell migration. Curr Biol 11, 918–930.

Alfandari D, McCusker C, Cousin H (2009). ADAM function in embryogenesis. Semin Cell Dev Biol 20, 153–163.

Alfandari D, Wolfsberg TG, White JM, DeSimone DW (1997). ADAM 13: a novel ADAM expressed in somitic mesoderm and neural crest cells during Xenopus laevis development. Dev Biol 182, 314–330.

Arima T, Enokida H, Kubo H, Kagara I, Matsuda R, Toki K, Nishimura H, Chiyomaru T, Tatarano S, Idesako T, *et al.* (2007). Nuclear translocation of ADAM-10 contributes to the pathogenesis and progression of human prostate cancer. Cancer Sci 98, 1720–1726.

Becker SF, Mayor R, Kashef J (2013). Cadherin-11 mediates contact inhibition of locomotion during Xenopus neural crest cell migration. PLoS One 8, e85717.

Borchers A, David R, Wedlich D (2001). Xenopus cadherin-11 restrains cranial neural crest migration and influences neural crest specification. Development 128, 3049–3060.

Chen X, Gumbiner BM (2006). Paraxial protocadherin mediates cell sorting and tissue morphogenesis by regulating C-cadherin adhesion activity. J Cell Biol 174, 301–313.

Cousin H, Abbruzzese G, Kerdavid E, Gaultier A, Alfandari D (2011). Translocation of the cytoplasmic domain of ADAM13 to the nucleus is essential for Calpain8-a expression and cranial neural crest cell migration. Dev Cell 20, 256–263.

Cousin H, Abbruzzese G, McCusker C, Alfandari D (2012). ADAM13 function is required in the 3 dimensional context of the embryo during cranial neural crest cell migration in Xenopus laevis. Dev Biol 368, 335–344.

Cousin H, Gaultier A, Bleux C, Darribere T, Alfandari D (2000). PACSIN2 is a regulator of the metalloprotease/disintegrin ADAM13. Dev Biol 227, 197–210.

de Carcer G, Manning G, Malumbres M (2011). From Plk1 to Plk5: functional evolution of polo-like kinases. Cell Cycle 10, 2255–2262.

de Melker AA, Desban N, Duband JL (2004). Cellular localization and signaling activity of beta-catenin in migrating neural crest cells. Dev Dyn 230, 708–726.

Descombes P, Nigg EA (1998). The polo-like kinase Plx1 is required for M phase exit and destruction of mitotic regulators in Xenopus egg extracts. EMBO J 17, 1328–1335.

Diaz-Rodriguez E, Montero JC, Esparis-Ogando A, Yuste L, Pandiella A (2002). Extracellular signal-regulated kinase phosphorylates tumor necrosis factor alpha-converting enzyme at threonine 735: a potential role in regulated shedding. Mol Biol Cell 13, 2031–2044.

Dinkel H, Van Roey K, Michael S, Davey NE, Weatheritt RJ, Born D, Speck T, Kruger D, Grebnev G, Kuban M, *et al.* (2014). The eukaryotic linear motif resource ELM: 10 years and counting. Nucleic Acids Res 42, D259–266.

Doble BW, Woodgett JR (2003). GSK-3: tricks of the trade for a multi-tasking kinase. J Cell Sci 116, 1175–1186.

Dominguez I, Itoh K, Sokol SY (1995). Role of glycogen synthase kinase 3 beta as a negative regulator of dorsoventral axis formation in Xenopus embryos. Proc Natl Acad Sci USA 92, 8498–8502.

Durocher D, Smerdon SJ, Yaffe MB, Jackson SP (2000). The FHA domain in DNA repair and checkpoint signaling. Cold Spring Harb Symp Quant Biol 65, 423–431.

Elia AEH, Rellos P, Haire LF, Chao JW, Ivins FJ, Hoepker K, Mohammad D, Cantley LC, Smerdon SJ, Yaffe MB (2003). The molecular basis for phosphodependent substrate targeting and regulation of Plks by the polo-box domain. Cell 115, 83–95.

Garcia-Castro MI, Marcelle C, Bronner-Fraser M (2002). Ectodermal Wnt function as a neural crest inducer. Science 297, 848–851.

Gaultier A, Cousin H, Darribere T, Alfandari D (2002). ADAM13 disintegrin and cysteine-rich domains bind to the second heparin-binding domain of fibronectin. J Biol Chem 277, 23336–23344.

Gawantka V, Ellinger-Ziegelbauer H, Hausen P (1992). Beta 1-integrin is a maternal protein that is inserted into all newly formed plasma membranes during early Xenopus embryogenesis. Development 115, 595–605.

Hammet A, Pike BL, McNees CJ, Conlan LA, Tenis N, Heierhorst J (2003). FHA domains as phospho-threonine binding modules in cell signaling. IUBMB Life 55, 23–27.

Harland RM (1991). In situ hybridization: an improved whole-mount method for Xenopus embryos. Methods Cell Biol 36, 685–695.

Ito J, Yoon SY, Lee B, Vanderheyden V, Vermassen E, Wojcikiewicz R, Alfandari D, De Smedt H, Parys JB, Fissore RA (2008). Inositol 1,4,5-trisphosphate receptor 1, a widespread Ca2+ channel, is a novel substrate of polo-like kinase 1 in eggs. Dev Biol 320, 402–413.

Izumi Y, Hirata M, Hasuwa H, Iwamoto R, Umata T, Miyado K, Tamai Y, Kurisaki T, Sehara-Fujisawa A, Ohno S, *et al.* (1998). A metalloprotease-disintegrin, MDC9/meltrin-gamma/ADAM9 and PKCdelta are involved in TPA-induced ectodomain shedding of membrane-anchored heparin-binding EGF-like growth factor. EMBO J 17, 7260–7272.

Jung B, Kohler A, Schambony A, Wedlich D (2011). PAPC and the Wnt5a/Ror2 pathway control the invagination of the otic placode in Xenopus. BMC Dev Biol 11, 36.

Kietzmann A, Wang Y, Weber D, Steinbeisser H (2012). Xenopus paraxial protocadherin inhibits Wnt/beta-catenin signalling via casein kinase 2beta. EMBO Rep 13, 129–134.

Koehler A, Schlupf J, Schneider M, Kraft B, Winter C, Kashef J (2013). Loss of Xenopus cadherin-11 leads to increased Wnt/beta-catenin signaling and up-regulation of target genes c-myc and cyclin D1 in neural crest. Dev Biol 383, 132–145.

Lander R, Nasr T, Ochoa SD, Nordin K, Prasad MS, Labonne C (2013). Interactions between Twist and other core epithelial-mesenchymal

transition factors are controlled by GSK3-mediated phosphorylation. Nat Commun 4, 1542.
Li Y, Sosnik J, Brassard L, Reese M, Spiridonov NA, Bates TC, Johnson GR, Anguita J, Visconti PE, Salicioni AM (2011). Expression and localization of five members of the testis-specific serine kinase (Tssk) family in mouse and human sperm and testis. Mol Hum Reprod 17, 42–56.
Liu KJ, Arron JR, Stankunas K, Crabtree GR, Longaker MT (2007). Chemical rescue of cleft palate and midline defects in conditional GSK-3beta mice. Nature 446, 79–82.
McCusker C, Cousin H, Neuner R, Alfandari D (2009). Extracellular cleavage of cadherin-11 by ADAM metalloproteases is essential for Xenopus cranial neural crest cell migration. Mol Biol Cell 20, 78–89.
McLennan R, Dyson L, Prather KW, Morrison JA, Baker RE, Maini PK, Kulesa PM (2012). Multiscale mechanisms of cell migration during development: theory and experiment. Development 139, 2935–2944.
Neuner R, Cousin H, McCusker C, Coyne M, Alfandari D (2009). Xenopus ADAM19 is involved in neural, neural crest and muscle development. Mech Dev 126, 240–255.
Petronczki M, Lenart P, Peters JM (2008). Polo on the rise—from mitotic entry to cytokinesis with Plk1. Dev Cell 14, 646–659.
Pohl BS, Knochel W (2004). Isolation and developmental expression of Xenopus FoxJ1 and FoxK1. Dev Genes Evol 214, 200–205.
Rizki A, Mott JD, Bissell MJ (2007). Polo-like kinase 1 is involved in invasion through extracellular matrix. Cancer Res 67, 11106–11110.
Santagati F, Rijli FM (2003). Cranial neural crest and the building of the vertebrate head. Nat Rev Neurosci 4, 806–818.
Schiffmacher AT, Padmanabhan R, Jhingory S, Taneyhill LA (2014). Cadherin-6B is proteolytically processed during epithelial-to-mesenchymal transitions of the cranial neural crest. Mol Biol Cell 25, 41–54.
Schwarz J, Schmidt S, Will O, Koudelka T, Kohler K, Boss M, Rabe B, Tholey A, Scheller J, Schmidt-Arras D, *et al*. (2014). Polo-like kinase 2, a novel ADAM17 signaling component, regulates tumor necrosis factor alpha ectodomain shedding. J Biol Chem 289, 3080–3093.
Soond SM, Everson B, Riches DW, Murphy G (2005). ERK-mediated phosphorylation of Thr735 in TNFalpha-converting enzyme and its potential role in TACE protein trafficking. J Cell Sci 118, 2371–2380.
Stuhlmiller TJ, Garcia-Castro MI (2012). Current perspectives of the signaling pathways directing neural crest induction. Cell Mol Life Sci 69, 3715–3737.
Sun T, Rodriguez M, Kim L (2009). Glycogen synthase kinase 3 in the world of cell migration. Dev Growth Differ 51, 735–742.
Tousseyn T, Thathiah A, Jorissen E, Raemaekers T, Konietzko U, Reiss K, Maes E, Snellinx A, Serneels L, Nyabi O, *et al*. (2009). ADAM10, the rate-limiting protease of regulated intramembrane proteolysis of Notch and other proteins, is processed by ADAMS-9, ADAMS-15, and the gamma-secretase. J Biol Chem 284, 11738–11747.
Wei S, Xu G, Bridges LC, Williams P, White JM, DeSimone DW (2010). ADAM13 induces cranial neural crest by cleaving class B Ephrins and regulating Wnt signaling. Dev Cell 19, 345–352.
Zanardelli S, Christodoulou N, Skourides PA (2013). Calpain2 protease: A new member of the Wnt/Ca(2+) pathway modulating convergent extension movements in Xenopus. Dev Biol 384, 83–100.